Towards optimal design parameters for around-the-end hydraulic flocculators

Johannes Haarhoff and Jeremia J. van der Walt

ABSTRACT

Hydraulic flocculators are principally characterized by their volume (which determines the time of flocculation) and the water level difference between inlet and outlet (which determines the average energy dissipation). Within these constraints, however, the designer has many degrees of freedom, such as the average water depth, the number and spacing of baffles, the length of the gap at the baffle ends, and the degree to which adjoining baffles overlap. In an earlier paper (Haarhoff 1998), these variables were systematically reduced to a number of critical ratios, and a comprehensive mathematical framework was presented whereby hydraulic flocculators can be designed once these ratios are fixed. In this paper, these ratios are further investigated by computational fluid dynamics (CFD) to find their optimal values. The validity of CFD modelling is first verified by comparing experimentally measured velocities in two flocculators against modelled velocities for similar hydraulic conditions. CFD is then used to systematically optimize the three critical design ratios for flocculator design. The optimal ratios are considered to be those that cause the least deviation from the average *G*-value; addressing the concern that there may be large *G*-value differences at different points in the flocculator.

Key words | baffled flocculators, computational fluid dynamics (CFD), hydraulic flocculation, velocity gradient

Johannes Haarhoff (corresponding author)
Department of Civil and Urban Engineering,
Rand Afrikaans University,
PO Box 524,
2006 Auckland Park,
South Africa
Fax: + 27 11 489 2148
E-mail: *jh@ing1.rau.ac.za*

Jeremia J. van der Walt
Magalies Water,
Private Bag X82327,
0300 Rustenburg,
South Africa

INTRODUCTION

Around-the-end hydraulic flocculators are widely used in many parts of the world, mainly due to their inherent simplicity and robust operation. Many designers, however, perceive them to be inflexible and not capable of maintaining a constant energy input under varying flow conditions. In a recent paper (Haarhoff 1998) it was shown that hydraulic flocculators are indeed capable of providing the desired operational flexibility, provided that the water depth in the flocculator can be adjusted. To prevent floc breakup, the adjustment has to done with an appropriate hydraulic control downstream of the sedimentation or flotation tank following the flocculator. Assuming shear flocculation to be the dominant mode of flocculation and a uniform energy dissipation rate throughout the flocculator, a comprehensive design methodology was developed to allow the detailed design and analysis of hydraulic flocculators, once a number of geometric ratios are chosen. However, an analysis of published design examples, and a full-scale plant survey in South Africa, indicated considerable variation in geometric ratios chosen in different parts of the world. It is therefore the purpose of this paper to:

- first demonstrate that computational fluid dynamics (CFD) will predict the flow behaviour in a hydraulic flocculator realistically;
- then utilize CFD to determine the variation in local energy dissipation, as well as the deviation from ideal plug flow for a range of geometric ratios; and finally
- suggest general guidelines for these geometric ratios to point designers towards more optimal designs.

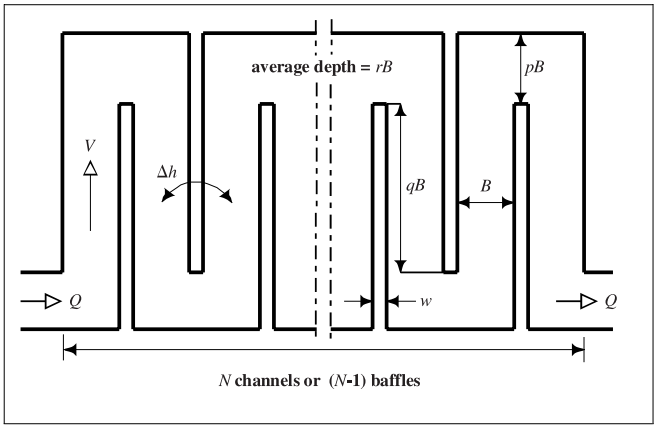

Figure 1 | Schematic layout of an around-the-end hydraulic flocculator, showing the notation used in this paper.

FLOCCULATOR GEOMETRY AND GEOMETRICAL RATIOS

A schematic plan of a hydraulic flocculator is shown in Figure 1, using identical baffles and constant baffle spacing throughout. In this paper the term 'flocculator' will be used for the entire reactor, and the term 'channel' for the sections between baffles. Five geometrical variables are required to define the plan layout of the flocculator:

N = number of channels, thereby fixing the number of baffles at $(N-1)$
B = the channel width between baffles
p = the slot width ratio (with respect to B)
q = the overlap ratio (with respect to B)
w = the baffle thickness

CONCEPTS, ASSUMPTIONS AND METHODOLOGY

The thinking underlying the current design methodology of hydraulic flocculators is built on a number of assumptions of which two are particularly prominent. One is that shear flocculation is the dominant mode of flocculation. The G-value therefore forms an integral part of the hydraulic flocculator design methodology. It is also assumed that a uniform G-value is desirable and feasible. A second assumption, relating to the degree of plug flow, assumes that the level of back-mixing is negligible. Intuitively it can be expected that real flocculators deviate from all these assumptions affecting the flocculator performance. The aim of this paper is to test the validity and practicality of these assumptions as follows:

- ***G*-value variation**: The absolute and relative spatial variation of G will be investigated first. The relative variation of G will be calculated by normalizing the absolute G-value with the average G-value. Performance indicators are proposed to simplify the interpretation of the relative variation. Finally the performance indicators are used to compare flocculators of different geometric proportions.
- **Backmixing**: The level of plug flow will be quantified by applying the Morrill Index (MI) and the dispersion coefficient (Di) to simulated residence time distribution (RTD) curves. The formulations used to calculate the indices are shown in Table 1.

The concept of the G-value needs to be clarified at this stage as the conventional interpretation can lead to confusion. The G-value is normally expressed as a function of the total energy input per total flocculator volume (Equation 1a), but it can also be expressed in terms of the total headloss and retention time (Equation 1b). The unit of G in both cases is: s^{-1}. The conventional interpretation of G is rather confusing as it is normally referred to as a velocity gradient, expressed in $m.s^{-1}.m^{-1}$.

The physical interpretation of the G-value is, however, not a velocity gradient, but rather the root mean energy dissipation rate per unit volume. The formulation used in this paper is given by Equation 1c:

$$G = \sqrt{\frac{P}{\mu V}} \quad (1a) \qquad G = \sqrt{\frac{gH}{\nu t}} \quad (1b) \qquad G = \sqrt{\rho \frac{\varepsilon}{\mu}} \quad (1c)$$

Table 1 | Performance indicator formulations (after Levenspiel, 1989)

Index	Formulation	
Morrill Index (MI)	$MI = \frac{T_{90}}{T_{10}}$	(2)
Dispersion Coefficient ($Di = 1/\mathrm{Pe}$)	$\frac{s^2}{\bar{t}^2} = \frac{2}{\mathrm{Pe}^2}[\mathrm{Pe} - 1 + \mathrm{e}^{-\mathrm{Pe}}]$	(3)
	where	
	$s^2 = \frac{2\sum_{i=1}^{n} t_i(C_{\max} - C_i)\Delta t_i}{\Delta C_{\max}} - \bar{t}^2$	(4)
	$\bar{t} = \frac{\sum_{i=1}^{n} (C_{\max} - C_i)\Delta t_i}{\Delta C_{\max}}$	(5)

Table 2 | Details of flocculators where measurements were taken

Parameter	Flocculator A	Flocculator B
Width B (mm)	860	680
Slot width (mm)	860	680
Water depth (mm)	880	935
Overlap (mm)	2,160	2,520
Slot width ratio	1.02	1.05
Depth ratio	1.05	1.44
Overlap ratio	2.57	3.88

EXPERIMENTAL VERIFICATION OF CFD SIMULATIONS

Background

In a recent paper (Van der Walt 1998) CFD was shown to have powerful potential for the analysis of hydraulic flocculators. Before CFD was used further to investigate flocculators in greater detail, it was considered necessary to first verify its predictions with practical measurements. Two full-scale hydraulic flocculators at the Vaalkop water treatment plant in the Northwest Province of South Africa were used for verification (see Table 2). The approach was to measure a number of velocity profiles in each channel, and then to do a CFD simulation of the same channels under identical operating conditions.

Measurement of velocity profiles

For both full-scale flocculators, the fourth turns were selected as representative. At each turn, five sections were located chosen as shown in Figure 2. A frame was firmly positioned above each section, from which an ÖTT turbine meter could be supported at any arbitrary point in the section. In Flocculator A velocities were measured

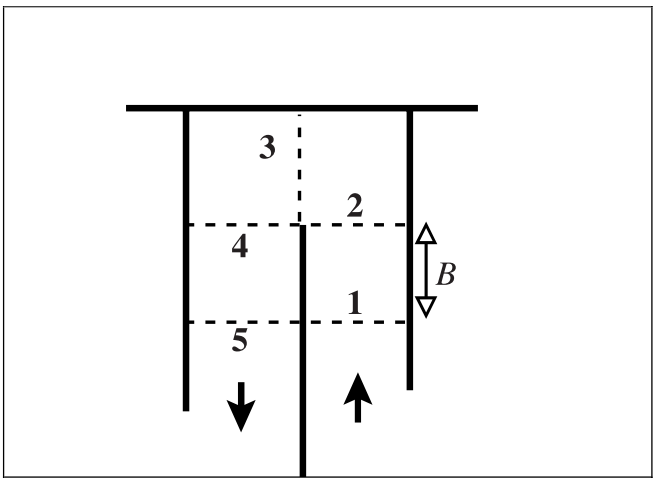

Figure 2 | Positions of experimental measurement sections.

at 35 points per section (7×5) and in Flocculator B, 36 points were measured per section (6×6), with a measurement period of at least 60 seconds per point. The meter was positioned at right angles to the sections shown in Figure 2.

Some practical problems were experienced during the measurements relating to flow reversal as the meter gave no indication of flow direction, increasing the pulse counts regardless of the flow direction. At some sections with very low flow, flow reversals occurred during the measurement period, which led to an over-estimation of the velocity. A further complication was that, due to high water turbidity, the flow meter impeller could not be seen

at progressive water depths. In general, however, a reliable profile could be measured, bar a few isolated outliers.

CFD simulation of velocity profiles

The turbulent flow in the flocculator was simulated with the Navier-Stokes equations and the standard $k-\varepsilon$ model. The SIMPLE algorithm (Patankar 1980) with a collocated grid and a conjugate gradient solver was employed by the Flo++ code (Le Grange 1999) to solve the Navier-Stokes equations and $k-\varepsilon$ turbulence model. An unsteady non-reactive tracer was simulated by linking a scalar equation to the momentum equations and solved using the PISO algorithm (Issa 1986).

The G-value for each cell of the computational grid was calculated using Equation 1. Clear water density and viscosity were used while the dissipation rate (ε) was obtained from solving the $k-\varepsilon$ turbulence model.

Comparison between CFD modelling and measurements

The experimental matrices (35 or 36 points per section), as well as the simulated matrices at each section (more than 200 points per section) were imported to ILWIS (a digital terrain modelling software package). As these matrices had different resolutions, values were interpolated with a moving average algorithm to a common resolution of 140 points per section to allow easy comparison (Otto 1998).

Visual comparison between the measured and simulated velocity contours provided convincing evidence that CFD provides a realistic approximation of the actual flow pattern. The measured *versus* the simulated velocity profiles of Flocculator B (velocities indicated in $mm.s^{-1}$) are shown as an example in Figure 3. There is thus good reason to believe that CFD will be an appropriate and reliable tool for the optimization of hydraulic flocculators, described in the rest of this paper.

OPTIMIZATION OF GEOMETRICAL RATIOS

Approach

CFD enables the designer to calculate the local G-value for each cell in the computational grid. In this case approximately 130,000 cells were used to model a flocculator with seven bends. The second last bend and straight section was chosen for the evaluation of the local G-values, as the flow was stabilized in this region and was not influenced by inlet conditions and the straight section near the outlet. The reference flocculator was selected with the average geometric ratios (Table 3), an average G-value of 50 and a uniform inlet velocity of 0.3 m/s.

Previous CFD analyses (Van der Walt 1998) considered the variation of the local G-values in a number of alternative flocculators. It was demonstrated that the slot width ratio, p, was the single most important geometrical parameter, and the depth ratio, q, the least important. The slot width ratio was therefore optimized first. The optimized slot width ratio was then fixed, followed by a similar optimization step for the overlap ratio. Finally, the optimized slot width and overlap ratios were fixed followed by an optimization step for the depth ratio.

The optimization was performed for a fixed baffle thickness of 200 mm, a fixed channel width of 700 mm, a flow rate of 40,000 $m^3.d^{-1}$ and a water temperature of 15°C. Each ratio was varied between the limits indicated in Table 3, using the average ratios as a starting point. These values represent an arbitrary range which the authors consider to be practical, based on an analysis of previously published and surveyed examples of hydraulic flocculators (Haarhoff 1998). The optimization was carried out by considering the two performance indicators identified in a previous section, namely the variation of G and the degree of backmixing.

VARIATION IN G

Inevitable variations of G are present in all flocculators, be they mechanical or hydraulic. An example of this spatial variation of G is shown in Figure 4, which is a plan section of the reference flocculator at mid-depth. The degree of shading indicates the G-value according to the legend shown on the figure. To obtain a more suitable quantitative description of this phenomenon, the absolute G-values are first normalized by dividing by the average G-value, and secondly presented as a percentile plot in Figure 5.

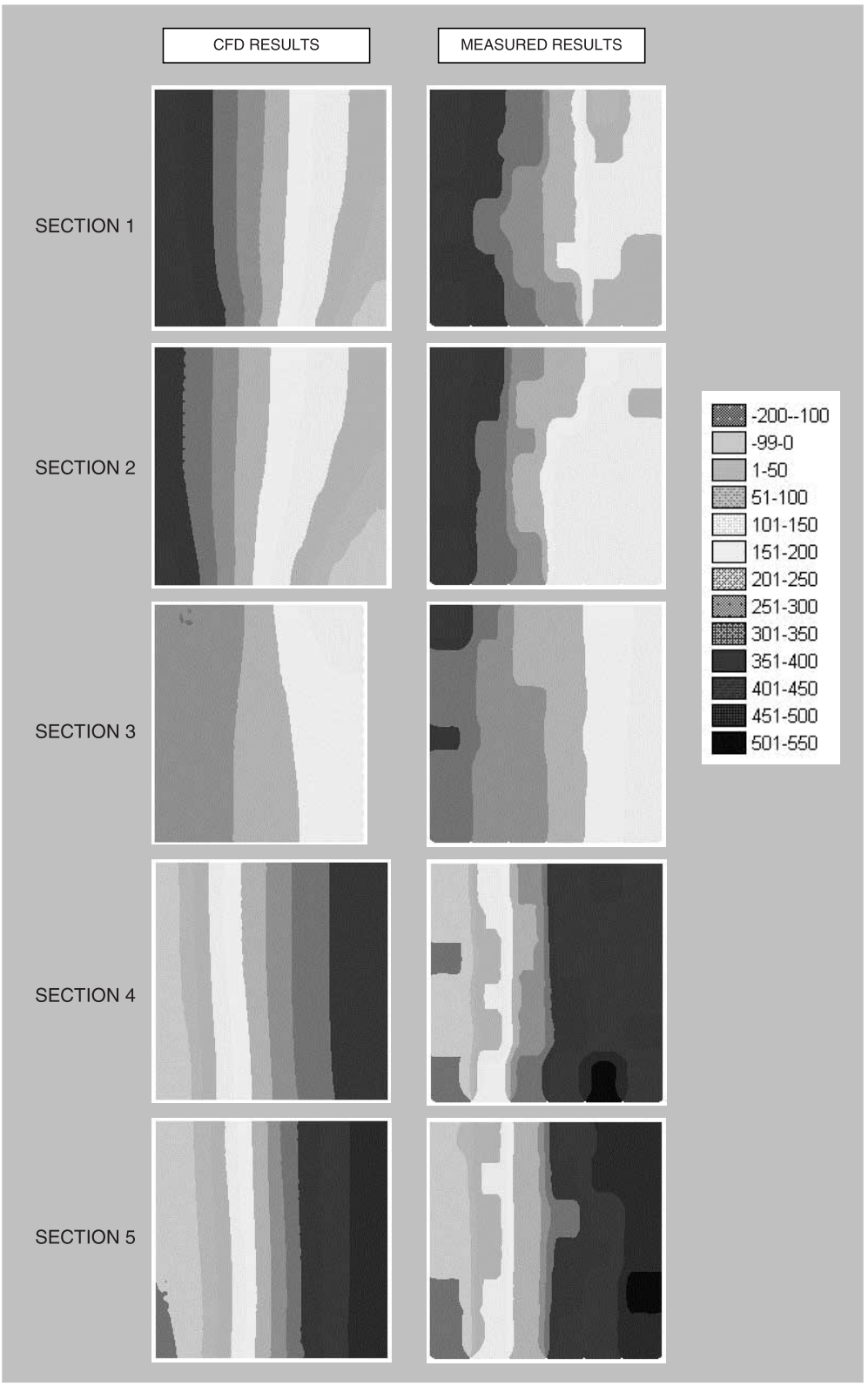

Figure 3 | Comparison of CFD calculated velocities and measured velocities.

Table 3 | Practical limits of geometrical ratios used for optimization

	Minimum	Average	Maximum	Order of optimization
Slot width ratio (p)	0.4	1.0	1.5	First
Overlap ratio (r)	1.5	4	10	Second
Depth ratio (q)	1.0	2.0	3.0	Last

As floc breakup in localized zones of excessively high turbulence is one of the major concerns during flocculation, a performance indicator is needed to limit the volume of these zones in a flocculator. The authors therefore propose the 95th percentile of the normalized G-value distribution in the flocculator as an arbitrary, but realistic, performance indicator with adequate sensitivity for the optimization process that follows. This 95th percentile normalized G-value is denoted by $\check{G}_{95}$.

Optimization of slot width ratio

To initiate the optimization process, a reference flocculator was used with the average geometric ratios, as described in Table 3. The CFD calculation was repeated for each of the 11 different slot width ratios.

The G_{95}-values for various slot width ratios are shown in Figure 6. It is evident that low slot width ratios (p-values) result in high G-values. This can be expected, as the same amount of fluid has to pass through a much smaller gap, resulting in higher velocities, velocity gradients and energy dissipation levels. This effect becomes less pronounced for larger slot width ratios, as the flow around the bend is not restricted by the baffle tip any longer, but deflected by the wall downstream of the turn.

The $\check{G}_{95}$-values are shown in Figure 7 and it can be seen that low and high slot width ratios result in high $\check{G}_{95}$-values. The lowest $\check{G}_{95}$-value is observed for a slot width ratio of one. The interpretation of both G_{95} and $\check{G}_{95}$ therefore results in the same conclusion of an optimal slot width ratio of unity.

Optimization of overlap ratio

The overlap ratio was changed next while the slot width ratio was kept at the optimal value ($p = 1$). The CFD calculations were repeated for each of the nine overlap ratios, ranging between the values listed in Table 3.

The $\check{G}_{95}$-values for different overlap ratios are shown in Figure 8. High overlap ratios result in high $\check{G}_{95}$-values. Overlap ratios of less than 5 result in normalized G-values of less than 1.5. The G_{95}-values for various overlap ratios (Figure 9), shows low G-values for high overlap ratios. This can be expected as larger areas of low velocity gradients are formed in longer channels. Low overlap ratios result in high G-values. Increasing the overlap ratio above 4 does not appear to increase the G-value any more. If both G_{95} and $\check{G}_{95}$ are taken into account it can be inferred that the optimal overlap ratio should be less than four.

Optimization of depth ratio

The depth ratio was finally optimized by keeping the slot width ratio and the overlap ratio constant at their respective optimal values ($p = 1$ and $q = 4$). The CFD calculations were repeated for five different depth ratios.

In the previous two geometric parameters the velocities at the inlet of the channel were kept constant to ensure the same mass flow into the flocculator. By varying the depth of the flocculator channel, for a given inlet velocity, the total mass flow rate can be varied. The approach used in this paper was to keep the average G-value as close as possible to 50 even if it meant the total mass flow was changed. This enables a fair comparison with other scenarios. This is slightly different from the approach used previously (Van der Walt 1998) where the same total mass flow was assumed, but the velocities at the inlet were adjusted.

Figure 10 shows only a marginal change in the normalized G-value when the depth ratio is changed. The same trend is observed for the absolute G-values. There is no clear optimum for the depth ratio within the range of values listed in Table 3. This means that the absolute G-values can be reduced by increasing the channel depth, but without affecting the G-value non-uniformity. The

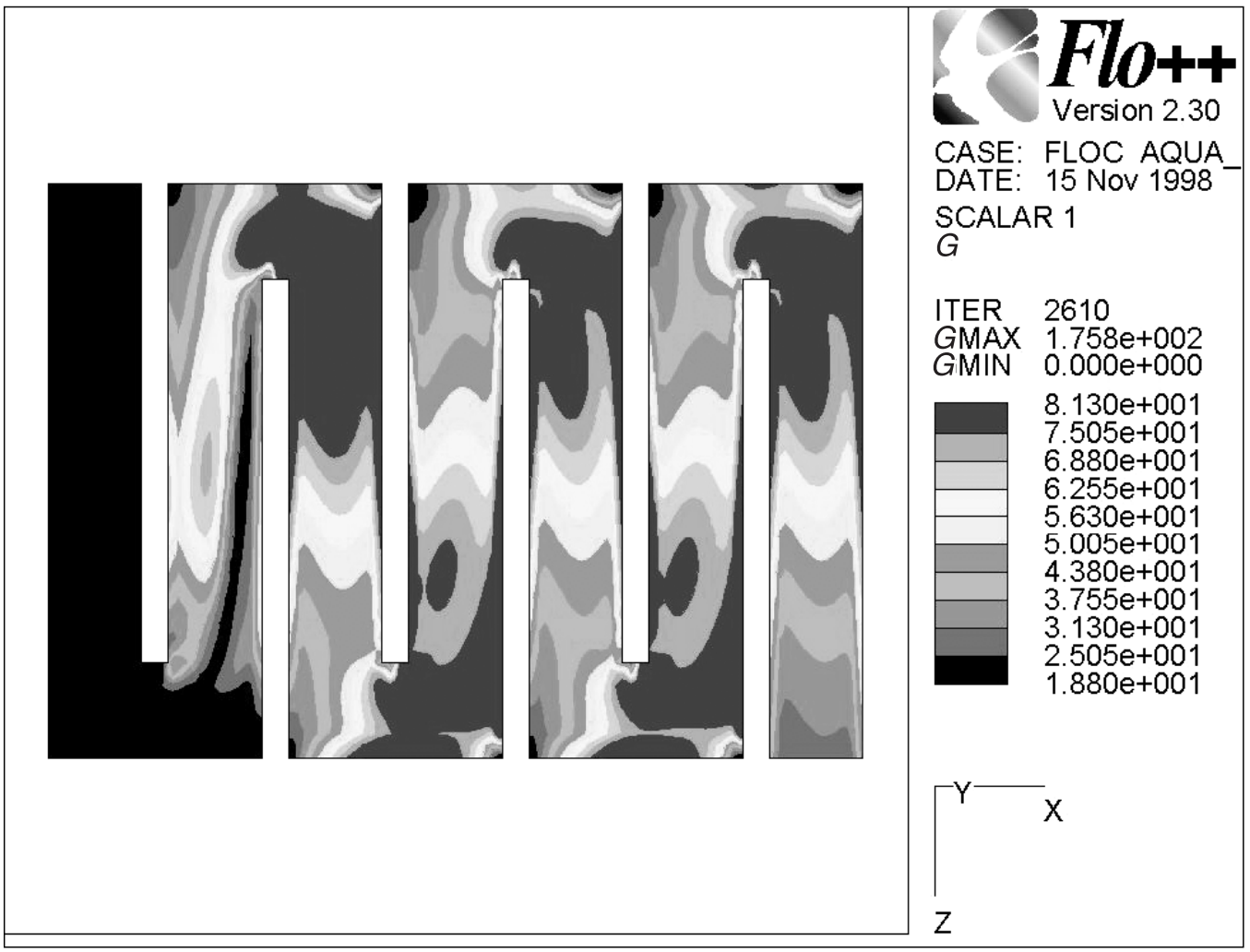

Figure 4 | Spatial variation of *G*-value at mid-depth for $p=1$, $q=4$, $r=2$.

benefits of increased operational flexibility when a fairly high depth ratio is used were pointed out earlier (Haarhoff 1998).

BACKMIXING

The level of backmixing was determined by evaluating a residence time distribution (RTD) generated by mathematically injecting a non-reactive tracer at the inlet. The RTD was evaluated by using T_{10}, T_{90}, MI and *Di*, where ideal plug flow will be reflected by a MI of 1 and a *Di* of 0.

Optimization of slot width ratio

The RTD curves for various slot width ratios are shown in Figure 11. It is clear that the T_{10} and T_{90} values for larger gap ratios are longer than for smaller gap ratios. In other words the effect of a change at the inlet takes longer to reach the outlet for a larger slot width ratio due to the increased total flocculator volume.

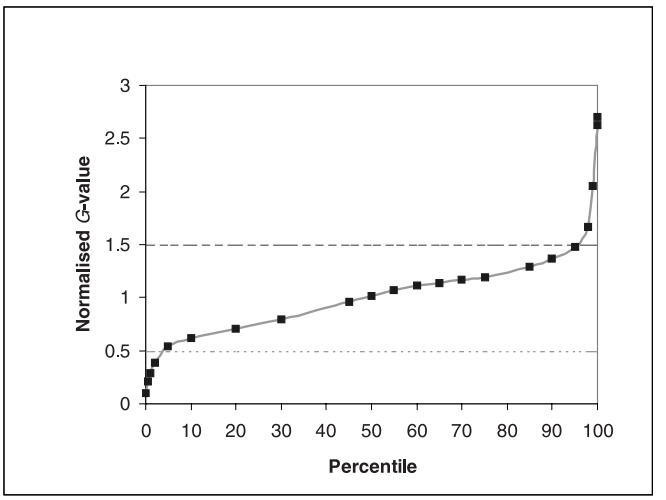

Figure 5 | Cumulative percentile distribution of normalized *G*-value in total flocculator volume.

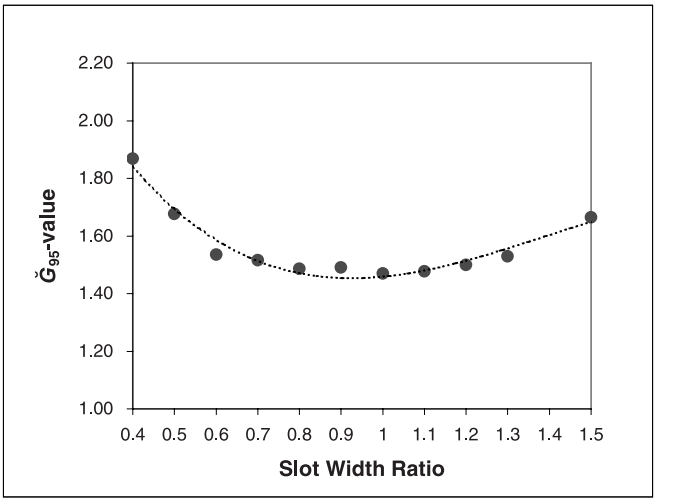

Figure 7 | $\check{G}_{95}$-values for various slot width ratios.

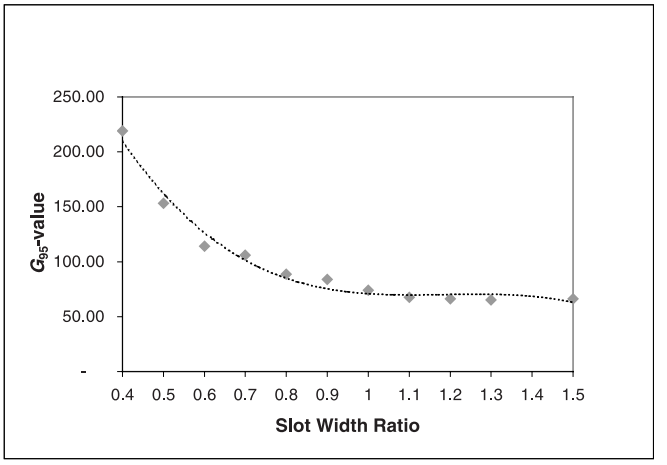

Figure 6 | G_{95}-values for different slot width ratios.

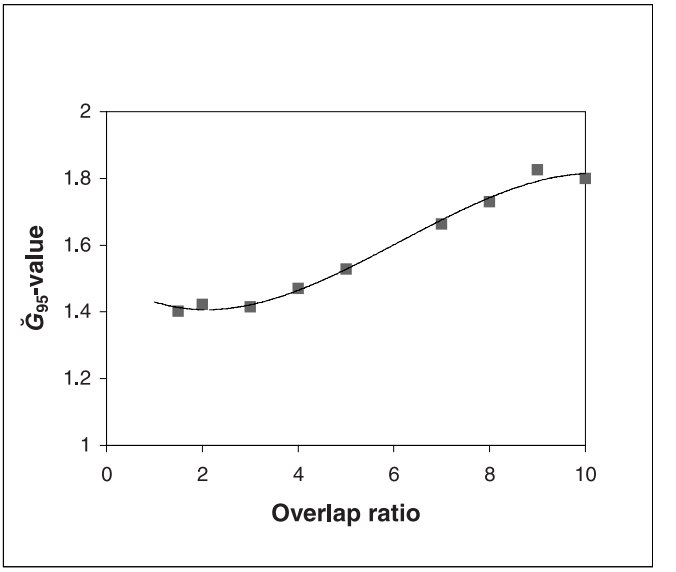

Figure 8 | $\check{G}_{95}$-values for various overlap ratios.

- It is clear from Figure 12 that higher slot width ratios approach plug flow conditions better than low slot width ratios. This is exhibited by both the MI and *Di* curves which exhibit a similar downward trend for higher overlap ratios. Little, however, is gained by using slot width ratios larger than 0.8.
- Since it is much easier to calculate the MI than the *Di* and since the *Di* does not provide any additional insight, only the MI will be calculated in subsequent paragraphs.

Optimization of overlap ratio

Figure 13 shows the Morrill Index for various overlap ratios. Larger overlap ratios approach plug flow better than lower overlap ratios due to better 'flow linearization' in the overlap sections. The MI does not change significantly beyond overlap ratios of 6.

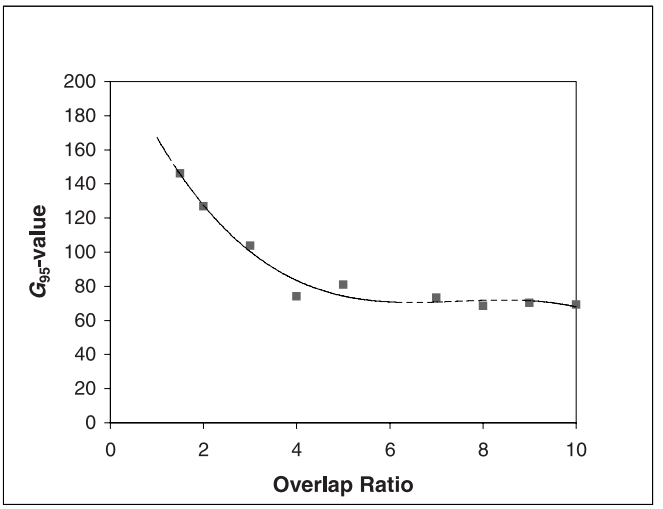

Figure 9 | G_{95}-values for different overlap ratios.

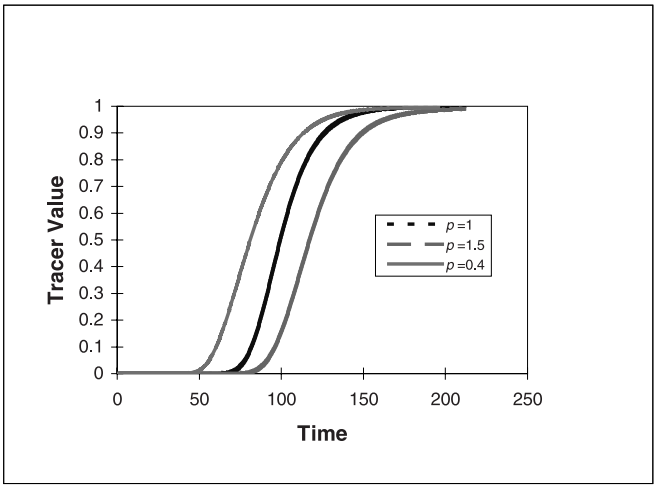

Figure 11 | RTD curves for various slot width ratios.

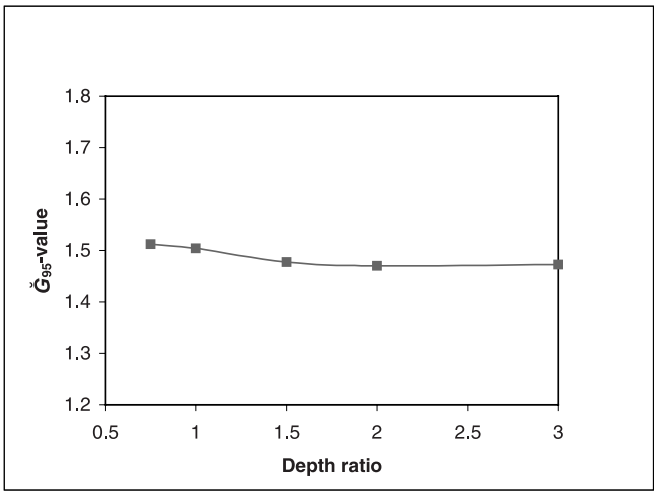

Figure 10 | $\check{G}_{95}$-values for various depth ratios.

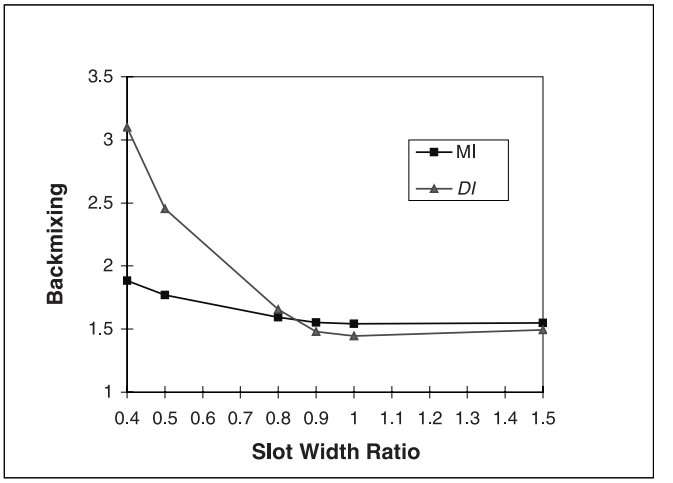

Figure 12 | Level of backmixing as reflected by MI and *Di* for various slot width ratios.

Optimization of depth ratio

The MI shows little change for the complete range of depth ratios evaluated. The level of backmixing is therefore also not very sensitive to the depth ratio.

DISCUSSION AND RECOMMENDATION

Analysis of the variation of G in a hydraulic flocculator provides new insight. The G_{95} and $\check{G}_{95}$ values enable the designer to compare the absolute and normalized G-values on a more representative basis than by simply using the average. These performance indicators need to be used simultaneously to provide the best guidance in selecting the ideal configuration.

The slot width ratio has the most significant effect on the local variation of G and it can also be argued that it will have the most detrimental impact on floccular efficiency if not selected with care. The overlap ratio has a less prominent effect on the local variation of G, but it also needs to be selected with care. The depth ratio, however,

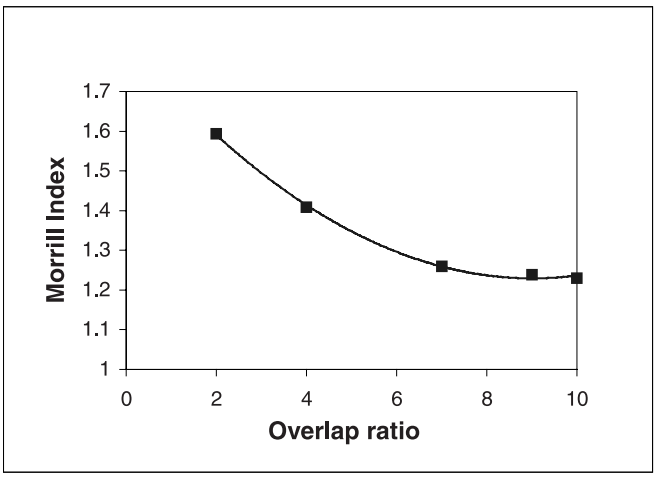

Figure 13 | Morrill Index for various overlap ratios.

Table 4 | Optimal geometrical ratios

	Optimum range G_{50}=50 s^{-1}
Slot width ratio	0.9–1.1
Overlap ratio	4–5
Depth ratio	1–3

does not have an impact on the local variation of *G* if the same channel velocity is maintained. The optimal solution found for a flocculator with a median *G*-value of 50 (± 50%) is listed in Table 4. Note that if the average value and the range change, the optimal geometric ratio will also change.

The level of backmixing provides insight from a different perspective, but it does not provide additional guidance in terms of the optimal geometric ratios. Optimal ratios recommended by analysing the variation of *G*-values were echoed by the MI and *Di* indices.

The optimum slot width ratio ranges from approximately 0.9 to 1.1 with an average of unity. Narrower slots cause a constriction with high local energy losses, while broader slots allow recirculation zones which increase backmixing.

The optimum overlap ratio lies in the region of 4 to 5. Lower values lead to more backmixing due to insufficient 'straightening' of the flow lines after a turn. Higher values lead to reduced backmixing, but lower levels of energy dissipation.

The depth ratio is almost unchanged throughout the range from about 1 to 3 normally encountered in practice. Designers are nevertheless urged to use depth ratios towards the higher end of this range, as a larger depth offers more operational flexibility in manipulating the velocity gradient should it be necessary.

SUMMARY AND CONCLUSIONS

Baffled hydraulic flocculators offer an attractive technology option for many parts of the world due to their inherent robustness and simplicity. With appropriate design and analysis, they also offer a degree of operational flexibility not commonly recognized. A previous paper (Haarhoff 1998) proposed a comprehensive design methodology, formulated in terms of three geometrical ratios. A survey of operational plants and examples from the literature showed that these ratios covered an extremely broad range. A subsequent paper (Van der Walt 1998) ranked these ratios in terms of their effects on flocculator performance; the slot width ratio being most important, followed by the overlap ratio and finally the depth ratio. In this paper, the following step was taken, namely to provide quantitative guidelines for each ratio for optimal flocculator performance.

CFD was used as an optimization tool. As a first step, practical velocity measurements were taken at numerous points in two different flocculators to enable the construction of velocity contours in different sections of the channels. The same hydraulic conditions were then modelled by CFD, and theoretical velocity contours were generated in the same sections. The agreement was excellent and CFD was used with confidence for the remainder of the study.

Two aspects of flocculator performance were considered. The first concern is the degree of variability in energy dissipation through the flocculator. Hydraulic

flocculators suffer from zones of high turbulence at the edges of the baffles (analogous to the zones of high turbulence at the tips and edges of mechanical impellers and paddles) which could induce floc breakup. This was quantified in this study by the G-value which is only exceeded in 5% of the total flocculator volume. The second concern is the degree of backmixing within the flocculator. This was quantified by simulating a RTD curve, from which the Morrill Index and Dispersion Coefficient could be calculated.

NOMENCLATURE

B	Channel width between baffles (m)
C	Concentration ($kg.m^{-3}$)
D	Water depth (m)
Di	Dispersion coefficient
g	Gravitational acceleration ($m.s^{-2}$)
G	G-value (s^{-1})
G_{50}	Median G-value (s^{-1})
G_{95}	95th percentile of G (s^{-1})
$\check{G}_{95}$	95th percentile of G normalized by G_{ave} (−)
H	Total headloss (m)
MI	Morrill Index (−)
N	Number of channels (−)
p	Slot width ratio, with respect to B (−)
P	Power input ($kg.m^2.s^{-3}$)
Pe	Peclet number (−)
q	Overlap ratio, with respect to B (−)
Q	Flow rate ($m^3.s^{-1}$)
r	Average water depth ratio, with respect to B (−)
s	Intermediate parameter used in the definition of Di
t	Flocculation time (s)
T	Temperature (°C)
u,v,w	Local channel velocity in x, y and z directions ($m.s^{-1}$)
U	Average channel velocity ($m.s^{-1}$)
V	Volume (m^3)
w	Baffle thickness (m)
ΔC_{max}	Maximum concentration difference ($kg.m^{-3}$)
Δh	Head loss across one turn (m)
ΔH	Head loss across the flocculator (m)
ΔS	Difference in floor level across the flocculator (m)
Δt	RTD time step (s)
ε	Dissipation rate of turbulent kinetic energy ($m^2.s^{-3}$)
ϱ	Density of water ($kg.m^{-3}$)
ν	Kinematic viscosity of water ($m^2.s^{-1}$)
μ	Dynamic viscosity of water ($kg.m^{-1}.s^{-1}$)

REFERENCES

Haarhoff, J. 1998 Design of around-the-end hydraulic flocculators. *Aqua* **47**(3), 142–152.

Issa, R. I. 1986 Solution of implicitly discretized fluid flow equations by operator-splitting. *J. Comp. Physics* **62**, 40–65.

Le Grange, L.A. 1999 *Flo + + User Manual* (unpublished). Potchefstroom. Available at *http://www.softlo.com*

Levenspiel, O. 1989 *The Chemical Reactor Omnibook*. Chemical Engineering Department, Oregon State University, Corvallis Oregon. Distributed by OSU Book Stores.

Otto, H. J. H. 1998 *Vloeipatrone in Kronkelkanale (Flow Patterns in Baffled Channels)*. Project Investigation for B.Eng degree, Rand Afrikaans University, South Africa.

Patankar, S. V. 1980 *Numerical Heat Transfer and Fluid Flow*. Hemisphere Publishing Corporation. New York. 197pp.

Van der Walt, J. J. 1998 The application of computational fluid dynamics in the calculation of local G values in hydraulic flocculators. *Proceedings of the Biennial Conference of the Water Institute of Southern Africa, 1998 Cape Town, South Africa*. Available at *http://www.wisa.co.za*